ACTA TECHNICA CORVINIENSIS – Bulletin of Engineering | e–ISSN: 2067 – 3809
Tome XIX [2026] | Fascicule 3 [July – September]

[1,2.] Adeolu Adesoji ADEDIRAN

OPTIMIZATION OF SQUEEZE CASTING PROCESSES IN THE FABRICATION OF ALUMINIUM–6063/15% SiC COMPOSITES

[1.] Materials Design & Structural Integrity Research Group, Department of Materials and Metallurgical Engineering, Federal University, Oye–Ekiti, Ekiti State, NIGERIA
[2.] Department of Mechanical Engineering Science, University of Johannesburg, SOUTH AFRICA

Abstract: Al6063/15 wt.% SiC is manufactured via the squeeze casting technique for use in engineering applications due to the benefits of squeeze casting over other casting methods. The procedure was optimized while response parameter prediction models were established on porosity, density, shrinkage, yield, and tensile strength, elongation, hardness, and impact strength. The influence of the process factors (squeeze pressure and moulding temperature) was analysed. The analysis of variance revealed that the two experimental inputs contributed significantly to the magnitude of all responses. The diagnostic plots generated for the models indicated that the models were highly compatible with the experimental results. In addition, surface plots demonstrated that responses were reliant on input elements and their interactions. The optimal performance of the composites may be attained by applying a squeezing pressure of 119.3 MPa at a molding temperature of 755.4 °C.
Keywords: aluminium composites; molten metal; silicon carbide; squeeze casting; squeeze pressure

INTRODUCTION

In engineering applications, metal composites comprising the reinforcement of metal matrices with particles have gained popularity due to their superior performance. They have been used in automobiles, airplanes, railroads, sports, etc., and they continue to be the subject of research. Aluminium metal composites use reinforcing phases such as whiskers and particles to strengthen an aluminium matrix. Ceramic particles are often employed to enhance the performance of composite aluminium alloys. Silicon carbide is a widely used ceramic particle (SiC).

The investigations of Rahman and Rashed [1] report the function of SiC as reinforcing phases in an aluminium matrix. In the investigation, SiC was injected at 0, 5, 10, and 20 wt.% into an aluminium matrix. It was noticed that porosity increased proportionally with the addition of additives. At 5, 10, and 15 wt.%, an increase in SiC fillers led to 58, 73, and 88 percent increases in hardness, respectively.

In a comparable context, Chando et al. [2] incorporated 10, 15, and 20 wt.% SiC into an aluminium matrix through stir casting. Porosity reduced linearly with particle addition, but density and hardness increased with particle addition, demonstrating that SiC may enhance composite densification and hardness. From the result of Yilmaz et al. [3], 1-3 wt.% SiC indicated a decrease in porosity as 5-7 wt. % SiC led to a rise in porosity. In this instance, when particle dosage rose from 1 to 3 wt.%, density improved, following which the density decreased when 5 to 7 weight percent of the particles were added. Using stir casting techniques, 3, 6, and 9 wt. % SiC was infused into the Cu alloy, causing a linear increase in Vickers hardness, yield strength, and ultimate tensile strength, and a gradual decrease in ductility [4].

In a similar fashion and by stir casting, Kumar et al. [5] demonstrated a linear increase in yield tensile, ultimate tensile, compressive, and hardness strengths when SiC was included into the Al2014 matrix at 0, 5, and 10 wt. %. Bandil et al. [6] demonstrated that the addition of SiC to an Al-Si alloy by stir casting technique improved its hardness, with a peak hardness of 15 wt. % addition. Hussain et al. [7] conducted experiments on the improvement of Al 6063 by using SiC in the proportions of 2, 4, 6, 8, and 10 wt. %. Observations revealed that the produced composite's hardness increased dramatically and linearly with increasing SiC filler concentrations. Similar results were reported for yield and ultimate tensile strength, although ductility decreased linearly with increasing SiC concentration.

According to the literature mentioned in the preceding paragraphs, stir casting was a primary approach for incorporating SiC particles into metal matrixes. Based on the difficulties associated with the stir casting method, namely porosity, this research focused on the use of the squeeze casting method. In squeeze casting, pressure is used during the casting process to reduce porosity, which often results in improved mechanical qualities. In this research, the casting procedure is derived from this premise. In addition, the examined research in the preceding paragraph focused largely on the influence of particle percentage on the produced composite without examining the effect of casting parameters on the composite's attributes. In this investigation, the effect of squeeze casting parameters (squeeze pressure and molding temperature) on the physical and mechanical characteristics of Al 6063/15 wt. % SiC was evaluated. 15 wt.% SiC was selected based on Bandil et al.'s [6] findings that Al 6063 exhibited maximal performance at 15 wt.% SiC addition.

The compression pressures (50, 100, and 150 MPa) and molding temperatures (700, 750, and 800 °C) were varied. Table 1 indicates the method in which the squeezing pressure (SP) and the molding temperature (MT) are combined for each experiment. The optimal parametric combination was determined using response surface analysis on the basis of the acquired experimental findings.

MATERIALS AND METHODS

Material and Casting Procedure

The materials include aluminium 6063 ingot and silicon carbide powder. The chemical composition by weight of the ingot as estimated by optical emission microscope is Al: 97.48, Mg: 0.83, Fe: 0.28, Si: 0.54, Cu: 0.12, Zn: 0.08, Ti: 0.1. After cleaning of the ingot, the ingot was charged into graphite crucible (initially preheated to 500 ℃) and heated to 750 ℃ until the charged ingot has melted.

The temperature of the crucible was monitored with the aid of a thermocouple. Preheated SiC particles (preheated at 500 ℃) were charged into the molten aluminium metal and stirring was done for 15 mins at 500 rpm to allow even dispersion. The obtained slurry was transferred into mould cavity of the die (initially preheated to 500 ℃) and the temperature was raised to 700, 750, and 800 ℃ at separate times (as indicated in Table 1).

Table 1: Variation in input variables for the experimental runs

Runs	Squeeze pressure (SP)	Moulding temperature (MT)
1	50	700
2	100	700
3	150	700
4	50	750
5	100	750
6	150	750
7	50	800
8	100	800
9	150	800

Varying squeeze pressure (50, 100, 150 MPa) was applied in discharging the slurry through a die maintained at 450 ℃ into the mould cavity. The castings were allowed to solidify in the air, after which demolding and fettling were carried out. Obtained casting samples were machined to varying dimensions required for the diverse tests.

Methods for Property Testing

Cylindrical samples of diameter 10 mm and height of 10 mm were used in the evaluation of the porosity, density, and hardness tests. The cast samples were sectioned into dimensions of 120 mm gauge length, 10 mm gauge diameter, and 100 mm gauge length for tensile samples.

— **Porosity and density**

Porosity and density were measured by Archimedes' principle according to ASTM B962-14. The initial weight of the samples in the air was measured. The weight of the samples while immersed in water was also measured. From the obtained results, the actual density of the samples was determined. For each experimental run, 4 samples were subjected to the test, and the average result was recorded. The theoretical density of the samples was evaluated by the mixture rule method, as indicated in equation (1).

$$\partial_t = [\partial_m \times (1 - V_r)] + (\partial_r \times V_r) \quad (1)$$

$\partial_t, \partial_m, \partial_r$ represent theoretical density of the composite, density of matrix and density of reinforcement respectively. Porosity is therefore evaluated employing equation (2).

$$\text{Porosity} = \left(1 - \frac{\partial_e}{\partial_t}\right) \times 100 \quad (2)$$

Where ∂_e is the estimated density from Archimedes principle, while ∂_t is the theoretical density.

— **Surface roughness measurement**

Surface roughness was measured using a surface roughness profiler (SJ-419) as per ASTM E 1274-18 [8] specifications. Three samples were tested for each experimental run, and the average value was recorded.

— **Tensile test**

The tensile test was conducted on a tensile sample employing a universal testing machine of model WAW 1000D by exposing the samples to a load of 100 kN at a strain rate of 4 x 10^{-3} s (ASTM E 8 [9]). Three samples were tested for each experimental run, and the average result was recorded. From the observed values, the yield and ultimate tensile strength as well as elongation were deduced for each experimental condition.

— **Hardness and impact strength**

The surfaces of the samples designated for hardness testing were polished until mirror like surfaces were obtained, and then they were subjected to the test using Vicker's microhardness tester, model MHT-1000T. The diamond pyramid was engaged at 136° in relation to ASTM E384 [10]. Seven indentations were made using a weight of 5 N and a duration of 15 sec for each indentation. The average result obtained for the seven indentations was recorded as the mean hardness value. Izod impact test was carried out in accordance with ASTM A370 [11] on samples of dimensions 55 x 10 x 10 mm^3 notched at 60˚ at the center of the sample. The notch was 2 mm deep. An Izod impact tester (model HT-5-50D-CM) was used for the test, and three samples representing each experimental run were tested, the average of which was taken as the mean impact energy for each run. The samples were clamped into the fixture of the equipment with the notched side facing the striking face of the pendulum. The pendulum is released from a striking distance of 180˚ to the center until a fracture occurred and the energy required for the fracture was noted.

RESULTS AND DISCUSSION

The experimental outcome for each run is as displayed in Table 2.

Table 2: Experimental values for the responses at varying experimental conditions

Runs	SP	MT	Po	Dn	SR	YS	UTS	El	HD	IS
1	50	700	2.45	2.67	1.3	174	202	9.7	76	10
2	100	700	2.12	2.75	1.1	195	232	9	84	16
3	150	700	1.86	2.86	0.93	213	253	8.3	92	13
4	50	750	2.14	2.73	1.21	213	251	9.1	82	16
5	100	750	1.8	2.8	1.02	236	284	8.4	90	22
6	150	750	1.54	2.94	0.82	254	301	7.6	98	19
7	50	800	1.81	2.78	1.08	194	233	8.7	86	13
8	100	800	1.52	2.86	0.93	214	262	8	94	19
9	150	800	1.23	2.98	0.7	232	280	7.2	102	16

SP and MT stands for squeeze pressure and moulding temperature respectively, while, Po, Dn, SR, YS, UTS, El, HD, IS stands for porosity, density, yield strength, ultimate tensile strength, elastic modulus, hardness, and impact strength respectively.

Statistical analysis of experimental results

As in previous studies by Olaniran et al. [12] and Akinwande et al. [13], experimental results were subjected to statistical analysis. An analysis of variance was carried out at a 95% confidence level to determine the significance of each experimental variable as well as its interactions. Also, mathematical models were derived for the prediction of the response properties as functions of the input variables. Equally, surface plots were used to express the trend of the responses as a function of the input variables. Lastly, an optimization procedure was undertaken to assess the optimum condition for balanced performance of the composite.

Analysis of Variance

The results of the ANOVA are presented in Table 3. From the table, the p values for factors A (squeeze pressure) and B (casting temperature) are less than 0.05, indicative of the fact that squeeze pressure and casting temperature are consequential with regard to all response parameters. Cross interactions between the factors demonstrated non-consequential influence on all the responses.

Table 3: Analysis of variances (ANOVA) on response

Source	Po	Dn	SR	YS	UTS	El	HD	IS
Model	< 0.0001	0.0005	0.0008	< 0.0001	< 0.0001	< 0.0001	< 0.0001	0.0020
A–Squeeze pressure	< 0.0001	< 0.0001	0.0002	< 0.0001	< 0.0001	< 0.0001	< 0.0001	0.0112
B–Casting Temp	< 0.0001	0.0005	0.0009	0.0002	< 0.0001	< 0.0001	< 0.0001	0.0102
AB	0.7663	0.5999	0.8116	0.6440	0.2071	0.1443	1.0000	0.1443
A^2	0.1049	0.0308	0.5152	0.0947	0.0065	0.1612	0.3081	0.0009
B^2	0.6767	0.3508	0.5152	< 0.0001	< 0.0001	0.0075	0.0917	0.0009
R^2	0.9763	0.9685	0.9795	0.9894	0.9876	0.9911	0.9792	0.9830

YS, UTS, El, HD, IS and FT stands for yield strength, ultimate tensile strength, elongation, hardness, impact strength and fracture toughness.

Equally, interaction A^2 portrayed a marginal effect on porosity, density, surface roughness, yield strength, elongation, and hardness, of which the interaction displayed significant roles on ultimate tensile strength, impact strength, and fracture toughness. As realized from the table, interaction B^2 reflected a substantial contribution to yield strength, ultimate tensile strength, elongation, impact strength, and fracture toughness, even though the contribution of the interaction on porosity, density, surface roughness, and hardness are insignificant. Since the p-values of interactions AB, A^2, and B^2 on porosity, density, and surface roughness are all less than 0.5, it shows that these factors are more dependent on the individual patterns of the input variables than their interactions. The coefficient of correlation R^2 with respect to all responses measured is greater than 0.95; therefore, the models are said to be statistically adequate to represent the data.

Figure 1 illustrates the probability plots of the property parameters, and as observed, the plotted data are distributed along the mean line, affirming a good relationship between the model and the data. The coefficient of correlation R^2 for each model is greater than 0.95, therefore, the models are affirmed to depict a good relationship between the predicted values and the experimental outcomes, and hence can be engaged in the prediction of the responses given the set variables. The models for the prediction of each response are expressed in equations (3) to (10).

$$Po = +8.3750 - 0.0087\,A - 0.0093\,B + 0.0000\,AB + 0.0000\,A^2 + 0.0000\,B^2 \qquad R^2 = 0.9763 \quad (3)$$

$$Dn = +0.4261 - 0.0062\,A + 0.0050\,B + 0.0000\,AB + 0.0000\,A^2 - 0.0000\,B^2 \qquad R^2 = 0.9685 \quad (4)$$

$$Sr = +0.5883 - 0.0023\,A + 0.0040\,B - 0.0000\,AB - 0.0000\,A^2 - 0.0000\,B^2 \qquad R^2 = 0.9795 \quad (5)$$

$$YS = -6863.0556 + 0.6017\,A + 18.6033\,B - 0.0001\,AB - 0.0007\,A^2 - 0.0123\,B^2 \qquad R^2 = 0.9894 \quad (6)$$

$$UTS = -7915.6667 + 1.2733\,A + 21.3333\,B - 0.0004\,AB - 0.0024\,A^2 - 0.0140\,B^2 \qquad R^2 = 0.9876 \quad (7)$$

$$El = +49.9722 - 0.0045\,A - 0.0793\,B - 0.0000\,AB - 0.0000\,A^2 + 0.0000\,B^2 \qquad R^2 = 0.9911 \quad (8)$$

$$HD = -150.2222 + 0.1333\,A + 0.5000\,B + 0.0000\,AB + 0.0001\,A^2 - 0.0003\,B^2 \qquad R^2 = 0.9792 \qquad (9)$$

$$IS = -1119.4444 + 0.5600\,A + 2.9433\,B - 0.0002\,AB - 0.0019\,A^2 - 0.0019\,B^2 \qquad R^2 = 0.9830 \qquad (10)$$

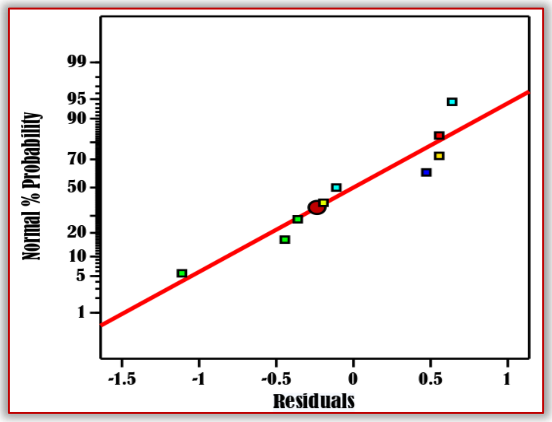

(a)

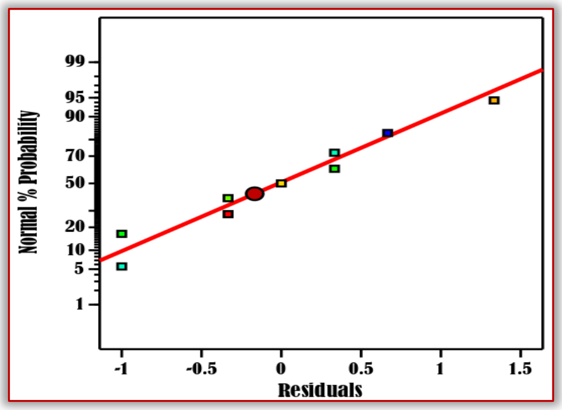

(b)

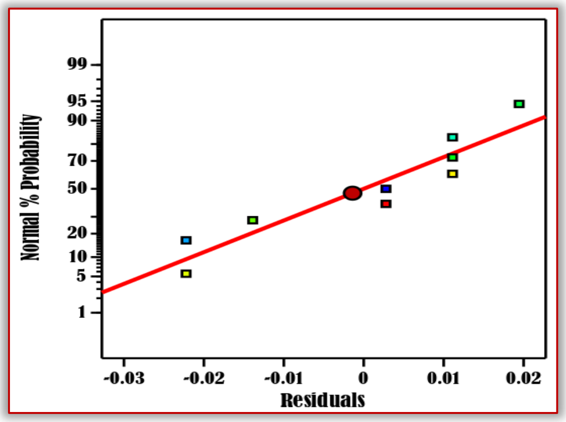

(c)

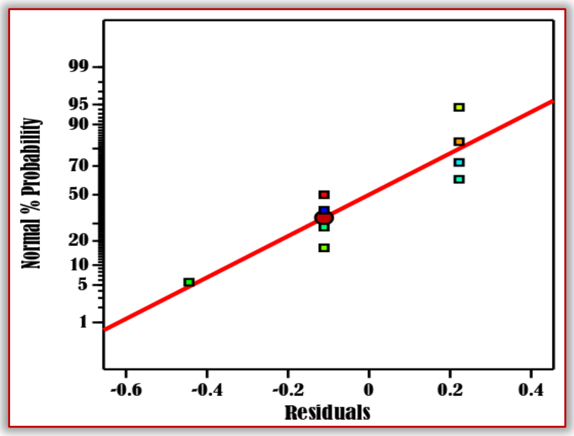

(d)

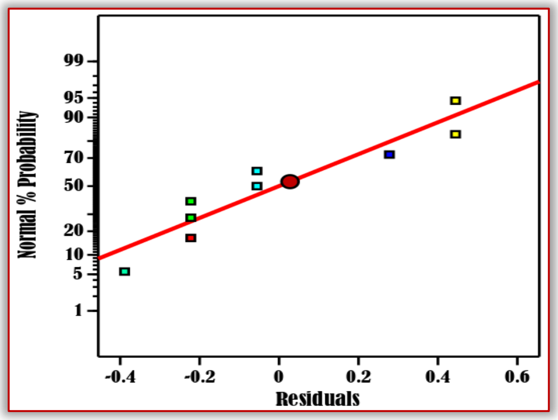

(e)

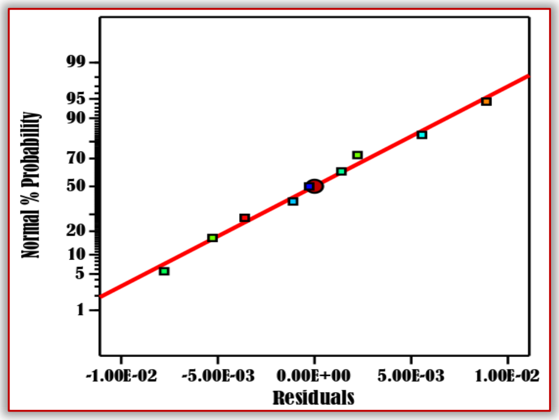

(f)

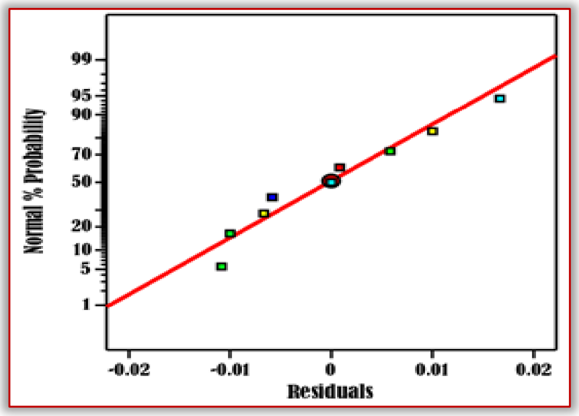

(g)

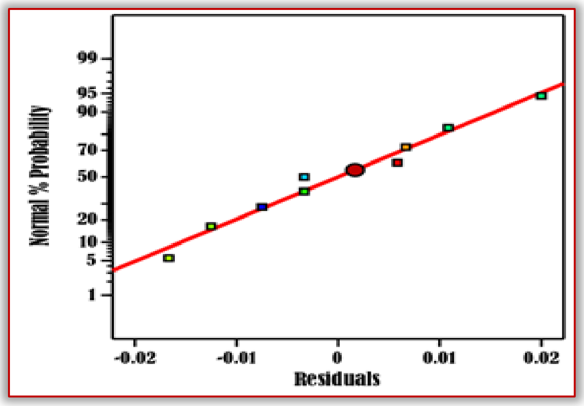

(h)

Figure 1: Probability plot of the properties parameter (a) porosity (b) density (c|) surface roughness (d) yield strength (e) ultimate tensile strength (f) elongation (g) hardness (h) impact strength.

Po, Dn, Sr, YS, UTS, El, HD, IS stands for porosity, density, yield strength, ultimate tensile strength, elastic modulus, hardness, and impact strength respectively

Response Analysis with Respect to the Input Variables

— **Porosity, density, and shrinkage**

The surface plot for porosity as a function of the input variables is indicated in Figure 2a. The plot showed that increasing squeeze pressure resulted in a decrease in porosity.

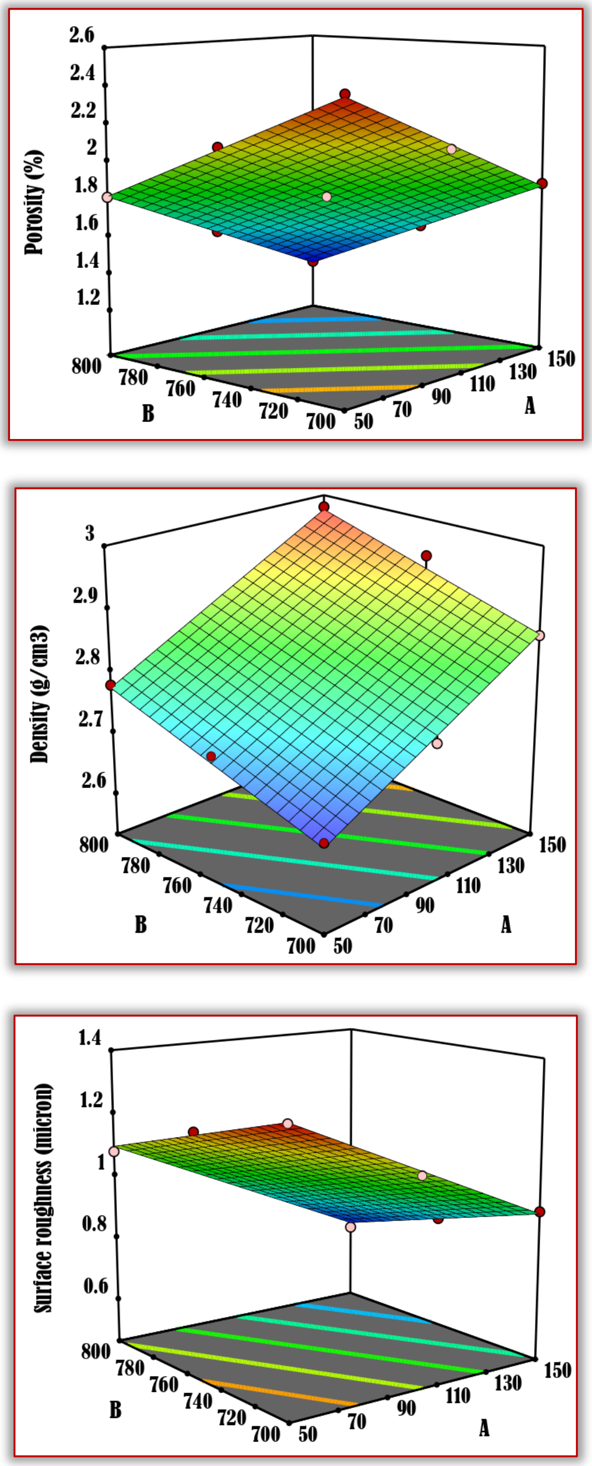

(a)

(b)

(c)

Figure 2: Property response of squeeze cast components (a) porosity (b) density (c) surface roughness.

This is based on the impact of the pressure application, which causes compaction within the melt and a decrease in porosity. Jahangiri et al. [14] revealed a direct linear decrease in porosity with applied pressure. In the same manner, Ozer et al. [15] reported reductions in porosity with rising pressure application. They associated the decrease with grain refinement and a decrease in gas or shrinkage porosities owing to pressure application. According to Li et al. [16], high pressure application during casting causes a decline in the nucleation of gas bubbles, thereby inhibiting gas porosity. More so, as a result of the improvement in the high compression of the metal liquid within the die based on high pressure application, shrinkage porosity is reduced. Equally, a rise in temperature accompanied a decline in porosity linked to the ease of flow at varying applied pressure occasioned by reduced viscosity. From Figure 2b, the density is depicted as increasing due to a decline in porosity as the pressure variable rose. Increased pressure application initiates a rise in cooling rate based on the enhancement of heat transfer obtained from the compression of the molten metal against the wall of the die. On the basis of this, porosity is reduced and equally enhanced compaction is realized, resulting in densification of the product. Temperature also contributed to density because of the lower viscosity during casting, resulting in ease of casting and improved densification within the cast product. The observation of Raji [17] revealed a slight rise in density between 650 and 700 °C molding temperatures and a progressive decrease in density with a rise in temperature from 700 to 850 °C. In Figure 2c, surface roughness decreased as both pressure and temperature increased. The findings reported in this study agree with the outcomes reported by Soundararajan et al. [18] and Ali et al. [19] in that increasing squeeze pressure triggered a reduction in surface roughness. The observation can be that with an increase in squeeze pressure, there is grain refinement that yields a finer microstructure based on solidification at high pressure. Also, higher temperatures induced higher fluidity in the liquid metal, hence a smoother surface.

— **Yield strength and ultimate tensile strength**

The surface plots of the property parameters are indicated in Figure 3. In Figures 3a and b, an increase in squeeze pressure between 50 and 150 MPa at pouring temperatures of 700 and 750 °C triggered improvements in yield and ultimate tensile strengths. Pressure contributed to the improvement in strength due to a reduction in porosity and an improvement in densification. As the temperature increases between 700 and 750 °C, the viscosity of the molten composite reduces, hence improving the flow rate as well as the compressibility as pressure is applied. As a result, there is an improvement in densification, resulting in improved mechanical properties. Souissi et al. [20] had shown how a linear increment in squeeze pressure resulted in a linear appreciation in the tensile strength performance of AA 6063, corroborating the findings revealed in this study. They attributed the improvement in tensile strength to a decrease in shrinkage, gas porosity, and grain refinement on account of the application of pressure. The findings of this report are in tandem with the outcomes of Raji and Khan [21] and Masoumi and Hu [22], who experience enhancement of tensile performance of squeeze-cast metal composites with increasing squeeze pressure. A decrease in strength between 700 and 750 °C can be associated with the existence of intermetallic phases as described in [22] and [23].

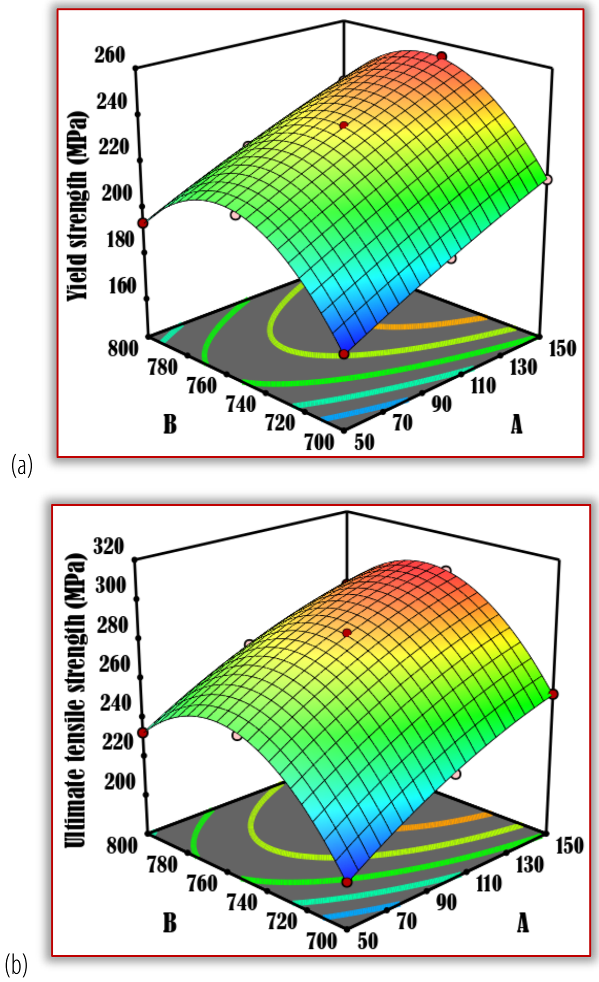

Figure 3: Interaction between the input variables on (a) yield strength (b) ultimate tensile strength

— Elongation and hardness

The response plots of elongation and hardness as functions of squeeze pressure and molding temperature are presented in Figures 4a and 4b. As demonstrated in Figure 4a, increasing pressure between 50 and 150 MPa at temperatures between 700 and 800°C reflected a linear decline in elongation. The observation is attributed to the improved densification with increased pressure and temperature application, eventually resulting in higher stiffness of the composite. As a result, there is increased resistance to tensile strain. The role of temperature is such that increasing temperature lowers viscosity and improves flow and compaction when applying pressure. It ensues well-structured lattice formation, yielding improved resistance to tensile strain. The revelation of Gurusamy and Prabu [25] affirms our findings, as they revealed a reduction in ductility as squeeze pressure increased. Contrarily, Yang et al. [26] showcased a progressive increase in ductility as pressure was increased between 0 and 150 MPa. In Figure 4b, increasing pressure application between 50 and 150 MPa ensued an enhancement of hardness. Increasing pressure ensues a high solidification rate and refinement of grains, with a consequent effect on the improvement of hardness [25]. The findings of authors Soundararajan et al. [27] demonstrated progressive improvement in hardness as applied pressure was increased from 70 to 140 MPa. This observation corroborates our findings. Equally, the results portrayed in the present study are in sync with the ones demonstrated by Klemens et al. [28], in which increasing the pouring temperature between 715 and 750 °C engendered improvements in hardness.

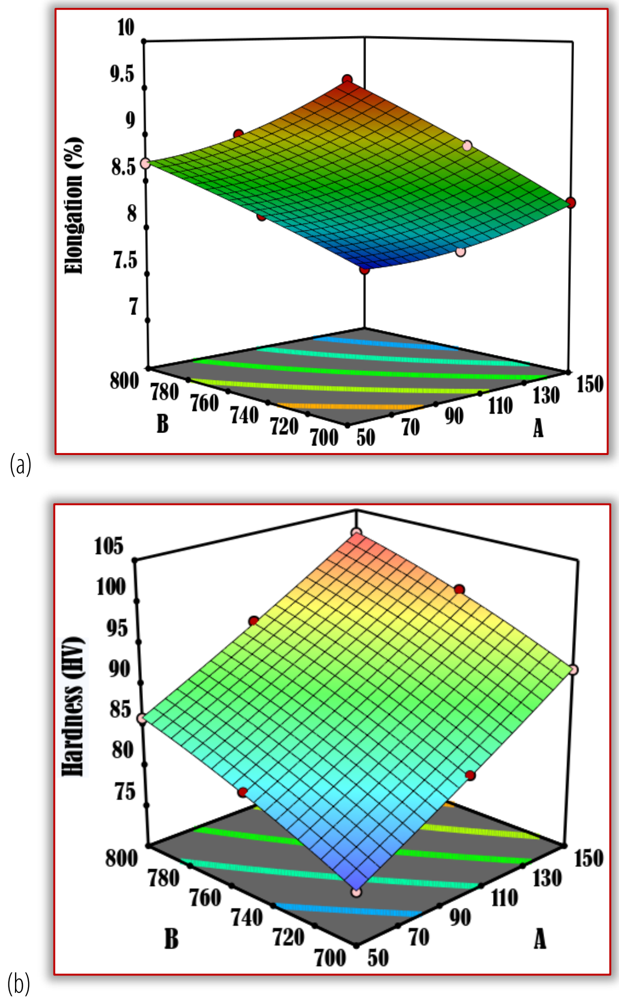

Figure 4: interaction between the input variables on (a) elongation (b) hardness

— Impact strength

The trend of impact strength with respect to the input variables is exhibited in Figure 5. As demonstrated in Figure 5, applied pressure in the range of 50 – 100 MPa at a pouring temperature of 700 – 750°C spurred enhancement of impact strength. The reportage of authors Azhagan et al.

[29] reflected a linear relationship between impact strength and applied pressure between 35 and 105 MPa, an observation similar to our findings between 50 and 100 MPa. In the same manner, Oladebeye et al. [30] noted an increasing linear relationship between applied pressure and impact strength of squeeze-cast 6063-aluminium. The chronicle of Zyska et al. [31] presents findings in tandem with our analysis in that 0 – 75 MPa of applied pressure triggered improvement in impact strength, of which 75 – 100 MPa caused a decrease in strength. The improvement in impact strength experienced between 50 and 100 MPa is hinged on improved compartmentalization initiated between particles, resulting in enhanced cohesion and reduced interparticle distance. More so, grain refinement must have contributed to the incurred impact strength via grain boundary strengthening. That notwithstanding, the decline in impact strength when pressure was increased beyond 100 MPa can be traced to stored residual stress that was induced as pressure increased, causing high staining within the matrix. Squeeze cast aluminium alloys (top section) fabricated by Yang [32] exhibited how temperatures of 660– 690 °C favored impact strength, while temperatures between 690 and 720 °C were detrimental to the strength. The assertion is consistent with the report presented in Figure 5a.

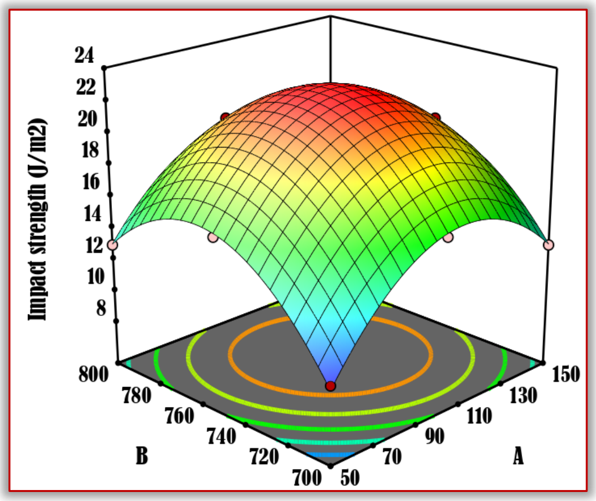

Figure 5: interaction between the input variables on impact strength

— Optimization and model validation

According to Balogun et al. [33]; Adediran et al. [34], optimization involves the process of deriving a single condition for achieving a balance of properties when analyzing a case involving more than one parameter expressed as a function of two or more experimental variables. This process has been described in several works of literature [35-40]. In the present report, response surface analysis was engaged in the optimization of the responses using the Design Expert 13 software. The criteria for the optimization procedure are spelled out in Table 4. The major objective was to maximize the strength parameters and minimize porosity, density, and surface roughness.

Table 4: Constraint for the optimization

Name	Goal	Lower Limit	Upper Limit	Importance
A: Squeeze pressure	is in range	50	150	3
B: Casting Temp	is in range	700	800	3
Po	minimize	1.23	2.45	3
Dn	minimize	2.67	2.98	3
SR	minimize	0.7	1.3	3
YS	maximize	174	254	3
UTS	maximize	202	301	3
El	maximize	7.2	9.7	3
HD	maximize	76	102	3
IS	maximize	10	22	3

Po, Dn, SR, YS, UTS, El, HD, IS, stand for porosity, density, surface roughness, yield strength, ultimate tensile strength, elongation, hardness, and impact strength

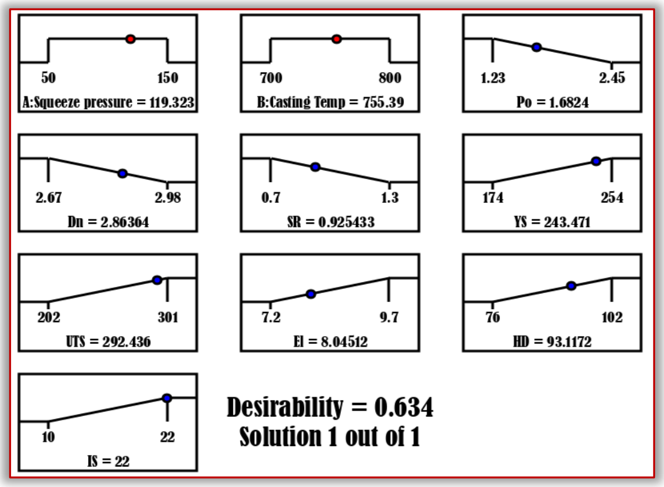

Figure 6: Optimization ramp

The optimal conditions for the response parameters are indicated in Figure 6, and they are 119.323 MPa for squeeze pressure and 755.39 °C for molding temperature. The predicted responses at predicted optimal parameters are 1.6824 %, 2.86464 g/cm^3, 0.925443 µm, 243.471 MPa, 292.436 MPa, 8.04512 %, 93.1172 HV, and 22 J for porosity, density, surface roughness, yield strength, ultimate tensile strength, elongation, hardness, and impact strength, respectively, at a desirability of 63.4%. A confirmation experiment was carried out by casting samples at optimal conditions of 119.3 MPa and 755.4 °C, which are approximate values for squeeze pressure and molding temperature. The confirmation result for each response was 1.67 %, 2.88 g/cm^3, 0.91 µm, 241.4 MPa, 294.8 MPa, 8.1, 92 HV, and 21.3 J for the respective responses, differing from the predicted response by values less than 5%. Going by the marginal deviation of the difference between the predicted values and the confirmation values for the responses, the models are confirmed to be adequate in the prediction of the response parameters.

CONCLUSION

In this study, the experimental values obtained in the squeeze casting of Al 6063/15 wt. % SiC were statistically analyzed for the purpose of developing mathematical regression in future forecasting of the responses and optimizing the input parameters. The followings were reached:

- Analysis of variance showed that the parameters: squeeze pressure and molding temperature played significant roles in the trend of all properties examined.
- The developed mathematical models for response prediction were determined to have a high degree of fitness with the experimental data.
- Increasing squeeze pressure and molding temperature resulted in a decrease in porosity and surface roughness but a rise in density.
- As regards the tensile strengths, increasing squeeze pressure between 50 and 150 MPa applied between 700 and 750˚C initiated improvements in yield and ultimate strengths, while the same pressure applied between 750 and 800˚C resulted in a decrease in the strengths.
- Meanwhile, 50 – 150 MPa of applied pressure at a molding temperature of 700 – 800˚C begets a progressive decline in elongation, even as the same values resulted in an enhancement of hardness.
- 50 to 100 MPa of pressure was favorable to the improvement of impact strength within a molding temperature range of 700 to 750 ˚C, whereas 100 to 150 MPa at temperatures of 750 to 800 ˚C is antagonistic to impact strength.

The optimization procedure predicted an optimum condition of 119.323 MPa for squeeze pressure and 755.39 ˚C for molding temperature. Confirmation experiments carried out at optimum conditions yielded responses whose deviations from the predicted values are insignificant, affirming the models to be adequate in the prediction of responses.

Acknowledgments

Adeolu Adesoji ADEDIRAN wish to thank the Council of Scientific and Industrial Research (CSIR), India, and The World Academy of Sciences (TWAS), Italy, for the CSIR–TWAS Postdoctoral Fellowship (Award No.22/FF/CSIR–TWAS/2022) to pursue his Postdoctoral Fellowship programme in CSIR–National Metallurgical Laboratory, Jamshedpur, India.

References

[1] M. H. Rahman, H. M. M. A. Rashed, Characterization of silicon carbide reinforced aluminium matrix composites. Procedia Engineering, 90, 103 – 109
[2] A. D. Chando, M. B. Ansari, S. Hussain, M. A. Siddiqui, 2019. Silicon carbide effect as reinforcement on aluminium metal matrix composites. Journal of the Chemical Society of Pakistan, 41(04), 650 – 655.
[3] O. Yilmaz, B. C. Turan, M. Gurbuz, 2019. Production and characterization of SiC reinforced aluminium composites from waste beverage cans. Journal of Metals, Materials, and Minerals, 29(4), 28 – 33.
[4] P. Samal, H. Tarai, A. Meher, B. Surekha, P. R. Vundavilli, 2023. Effect of SiC and WC reinforcements on microstructural and mechanical characteristics of copper alloy –based metal matrix composites using stir casting route. Applied Sciences, 13, 1754
[5] H. S. V. Kumar, K. Revanna, N. Kumar, N. Sathyanarayana, N. Madeva, G. A. Manjunath, H. Adisu, 2022. Impact of silicon carbide particles weight percentage on the microstructure, mechanical behavior, and fractography of Al2014 alloy composites. Advances in Materials Science and Engineering, 2022(2839150), 1 – 10.
[6] K. Bandil, H. Vashisth, S. Kumar, L. Verma, A. Jamwal, D. Kumar, N. Singh, K. K. Sadasivuni, P. Gupta, 2019. Microstructural, mechanical and corrosion behavior of Al–Si alloy reinforced with SiC metal matrix composite. Journal of Composite Materials, 0(0), 1 – 9.
[7] S. A. Hussain, R. Rajaneesh, H. Nizam, K. Jithin, 2019. Experimental analysis on aluminium alloy (6063) with silicon carbide: an experimental investigation. International Research Journal of Engineering and Technology, 6(10), 1 – 7. https://www.irjet.net/archives/V6/i10/IRJET–V6I1016.pdf
[8] ASTM E1274–18, 2018. Standard test method for measuring pavement roughness using a profilograph. ASTM International, PA. https://www.astm.org/e1274–18.html
[9] ASTM E 8, 2022. Standard test methods for tension testing of metallic materials. ASTM International, PA. https://www.astm.org/e0008_e0008m–22.html
[10] ASTM E384, 2022. Standard test method for microindentation hardness of materials. ASTM International, PA. https://blog.ansi.org/astm–e384–22–microindentation–hardness–test–method/
[11] ASTM A370, 2022. Standard test methods and definitions for mechanical testing of steel. Products. ASTM International, PA.
[12] O. Olaniran, A. A. Akinwande, A. A. Adediran, T. C. Jen, 2022. Process maps and regression models for the physio–thermo–mechanical properties of sintered Al–7075–molybdenum composite. Materials Letters
[13] A. A. Akinwande, O. A. Balogun, V. Romanovski, H. Danso, M. Kamarou, A. O. Ademati, 2022. Mechanical performance and Taguchi optimization of kenaf fiber/cement–paperboard composite for interior application. Environmental Science and Pollution Research, 29, 52675–52688.
[14] A. Jahangiri, S. P. H. Marashi, M. Mohammadaliha, V. Ashofte, 2017. The effect of pressure and pouring temperature on the porosity, microstructure, hardness, and yield stress of AA 2024 aluminium alloy during the squeeze casting process. Journal of Materials Processing Technology, 245, 1 – 6.
[15] G. Ozer, K. A. Guler, H. MM. Lus, 2012. Effects of squeeze pressure on microstructure, porosity and hardness of an in–situ Mg2Si/Al–Si–Cu composite. Materials Testing, 54(1), 26 – 29.
[16] J. Li, Y. Pan, D. Zhao, S. Lu, S. Wu, W. Guo, 2022. Development of a novel high strength and toughness Al–Cu–Li alloy casting billet with a new process. Materials Science and Engineering: A, 854, 143827.
[17] A. Raji, 2005. Effect of pouring temperature on the properties of Al–8%Si alloy sand cast components. Global Journal of Engineering Research, 4(1–2), 1 – 4
[18] R. Soundararajan, P. Saravanakumar, P. M. Sendil, A. Ramesh, K. M. Rajasekaran, 2018. Effect of squeeze cast process parameter on surface roughness of A413–B4C composites. International Journal of Mechanical and Production Engineering Research and Development, 8(2), 1157 – 1166

[19] M. A. Ali, K. Ishfaq, M. Jawad, 2019. Evaluation of surface quality and mechanical properties of squeeze casted AA2026 aluminium alloy using response surface methodology. The International Journal of Advanced Manufacturing Technology, 103, 4041 – 4054.

[20] S. Souissi, H. Barhoumi, M. B. Amar, F. Elhalouani, 2019. Microstructure evolution and mechanical properties of the T6 heat treated AA6063 alloy produced by squeeze casting. Physics of Metals and Metallography, 120(8), 806 – 812.

[21] A. Raji, R. H. Khan, 2006. Effects of pouring temperature and squeeze pressure on Al–8%Si alloy squeeze cast parts. AU J. T. 9(4), 229 – 237. Available at https://www.researchgate.net/publication/237344437

[22] M. Masoumi, H. Hu, 2011. Influence of applied pressure on microstructure and tensile properties of squeeze cast magnesium Mg–Al–Ca alloy. Materials Science and Engineering A, 528, 3589 – 3593.

[23] O. S. Adesina, A. A. Akinwande, O. A. Balogun, A. A. Adediran, O. O. Sanyaolu, V. Romanovski, 2023. Statistical analysis and optimization of the experimental results on performance of green aluminium–7075 hybrid composites. Journal of Composites Science, 7(3), 115.

[24] A. A. Akinwande, O. S. Adesina, A. A. Adediran, O. A. Balogun, D. Mukuro, O. P. Balogun, K. F. Tee, M. S. Kumar, 2023. Microstructure, process optimization, and strength response modelling of green–aluminium–6061 composite as automobile material. Ceramics, 6, 386 – 415.

[25] P. Gurusamy, S. B. Prabu, 2013. Effect of the squeeze pressure on the mechanical properties of the squeeze cast Al/SiC_p metal matrix composites. International Journal of Microstructure and Materials Properties, 8(4/5), 299 – 312.

[26] L. Yang, H. Hou, Y. Zhao, X. Yang, 2015. Effect of applied pressure on microstructure and mechanical properties of Mn–Zn–Y quasicrystal–reinforced AZ91D magnesium matrix composites prepared by squeeze casting. Transaction of Nonferrous Metals Society of China, 25, 3936 – 3943.

[27] R. Soundararajan, A. Ramesh, S. Sivasankaran, A Sathishkumar, 2015. Modeling and analysis of mechanical properties of aluminium alloy (A413) processed through squeeze casting route using artificial neural network model and statistical technique. Advances in Materials Science and Engineering, 2015(714762), 1 – 16.

[28] A. R. Klemens, F. S. Cipto, M. Syahid, 2019. Study on effect of temperature smelting and pouring to mechanical properties aluminium 7075. IOP Conference Series: Earth and Environmental Science, 343, 012166.

[29] M. T. Azhagan, B. Mohan, A. Rajadurai, S. Maharajan, 2014. Influence of squeeze pressure on the mechanical properties of squeeze cast aluminium alloy AA6061. Advanced Materials Research, 984–985, 350 – 354.

[30] D. H. Oladebeye, E. R. Adefidipe, O. Awogbemi, 2021. Effect of impact and fatigue test on cast 6063 aluminium rods produced from sand and squeeze cast moulds. International Journal of Scientific Engineering and Applied Science, 7(12), 18 – 26. https://ijseas.com/volume7/v7i12/IJSEAS202112103.pdf

[31] A. Zyska, Z. Konopka, M. Lagiewka, 2020. Impact strength of squeeze casting $AlSi13Cu2–C_F$ composite. Archives of Foundry Engineering, 2020, 49 – 52

[32] L. J. Yang, 2003. The effect of casting temperature on the properties of squeeze cast aluminium and zinc alloys. Journal of Materials Processing Technology, 140 (1–3), 391–396

[33] O. A. Balogun, A. A. Akinwande, O. A. Ogunsanya, A. O. Ademati, T. J. Erinle, E. Akinlabi, 2022. Central composite design and optimization of selected stir casting parameters on flexural strength and fracture toughness $mTiO_{2p}$/Al 7075 composites. Materials Today: Proceedings. 62(6), 4574–4583.

[34] A. A. Adediran, A. Akinwande, O. A. Balogun, O. S. Bello, M. K. Akinbowale, O. S. Adesina, A. A. Ojo, 2022. Mechanical and optimization studies of polypropylene hybrid biocomposites. Scientific Reports, 12, 2468

[35] O. Ogunbiyi, Y. Tin, A. A. Akinwande, A. L. Rominiyi, 2023. AA7075/HEA composites fabricated by microwave sintering: Assessment of the microstructural features and response surface optimization. Intermetallics, 155, 107830.

[36] A. A. Akinwande, O. A. Balogun, A. A. Adediran, O. S. Adesina, V. Romanovski, T. C. Jen, 2022. Experimental analysis, statistical modeling, and parametric optimization of quinary–$(CoCrFeMnNi)_{100-x}/TiC_x$ high–entropy–alloy (HEA) manufactured by laser additive manufacturing. Results in Engineering, 17, 100802.

[37] A. A. Akinwande, D. O. Folorunso, O. A. Balogun, H. Danso, V. Romanovski, 2022. Paperbricks produced from wastes: modeling and optimization of compressive strength by response surface approach. Environmental Science and Pollution Research.

[38] A. O. Ademati, A. A. Akinwande, O. A. Balogun, V. Romanovski, 2022. Optimization of bamboo fiber–reinforced composite–clay bricks for development of low–cost farm settlements toward boosting rural agribusiness in Africa. Journal of Materials in Civil Engineering, 34(12), 04022335.

[39] O. S. Adesina, A. A. Adediran, A. A. Akinwande, O. O. Daramola, O. O. Sanyaolu, 2022. Modeling and optimizing tensile behavior of developed aluminium hybrid composite. Surface Review and Letters.

[40] A. A. Akinwande, D. O. Folorunso, O. A. Balogun, V. Romanovski, 2022. Mathematical modelling, multi–objective optimization, and compliance reliability of paper–derived eco–composites.

ISSN: 2067–3809